JB Journals.ASM.org

Heterotrimeric NADH-Oxidizing Methylenetetrahydrofolate Reductase from the Acetogenic Bacterium *Acetobacterium woodii*

Johannes Bertsch,[a] Christian Öppinger,[a] Verena Hess,[a] Julian D. Langer,[b] Volker Müller[a]

Molecular Microbiology & Bioenergetics, Institute of Molecular Biosciences, Johann Wolfgang Goethe University Frankfurt/Main, Frankfurt, Germany[a]; Max Planck Institute for Biophysics, Frankfurt, Germany[b]

ABSTRACT

The methylenetetrahydrofolate reductase (MTHFR) of acetogenic bacteria catalyzes the reduction of methylene-THF, which is highly exergonic with NADH as the reductant. Therefore, the enzyme was suggested to be involved in energy conservation by reducing ferredoxin via electron bifurcation, followed by Na^+ translocation by the Rnf complex. The enzyme was purified from *Acetobacterium woodii* and shown to have an unprecedented subunit composition containing the three subunits RnfC2, MetF, and MetV. The stable complex contained 2 flavin mononucleotides (FMN), 23.5 ± 1.2 Fe and 24.5 ± 1.5 S, which fits well to the predicted six [4Fe4S] clusters in MetV and RnfC2. The enzyme catalyzed NADH:methylviologen and NADH:ferricyanide oxidoreductase activity but also methylene-tetrahydrofolate (THF) reduction with NADH as the reductant. The NADH:methylene-THF reductase activity was high (248 U/mg) and not stimulated by ferredoxin. Furthermore, reduction of ferredoxin, alone or in the presence of methylene-THF and NADH, was never observed. MetF or MetVF was not able to catalyze the methylene-THF-dependent oxidation of NADH, but MetVF could reduce methylene-THF using methyl viologen as the electron donor. The purified MTHFR complex did not catalyze the reverse reaction, the endergonic oxidation of methyl-THF with NAD^+ as the acceptor, and this reaction could not be driven by reduced ferredoxin. However, addition of protein fractions made the oxidation of methyl-THF to methylene-THF coupled to NAD^+ reduction possible. Our data demonstrate that the MTHFR of *A. woodii* catalyzes methylene-THF reduction according to the following reaction: NADH + methylene-THF → methyl-THF + NAD^+. The differences in the subunit compositions of MTHFRs of bacteria are discussed in the light of their different functions.

IMPORTANCE

Energy conservation in the acetogenic bacterium *Acetobacterium woodii* involves ferredoxin reduction followed by a chemiosmotic mechanism involving Na^+-translocating ferredoxin oxidation and a Na^+-dependent F_1F_o ATP synthase. All redox enzymes of the pathway have been characterized except the methylenetetrahydrofolate reductase (MTHFR). Here we report the purification of the MTHFR of *A. woodii*, which has an unprecedented heterotrimeric structure. The enzyme reduces methylene-THF with NADH. Ferredoxin did not stimulate the reaction; neither was it oxidized or reduced with NADH. Since the last enzyme with a potential role in energy metabolism of *A. woodii* has now been characterized, we can propose a quantitative bioenergetic scheme for acetogenesis from H_2 plus CO_2 in the model acetogen *A. woodii*.

Acetogenic bacteria are a group of strictly anaerobic bacteria that can grow lithoautotrophically by reduction of carbon dioxide with molecular hydrogen to acetate (1, 2). CO_2 is reduced in the Wood-Ljungdahl pathway, which is the only pathway known to combine CO_2 fixation with the synthesis of ATP (3–5). CO_2 reduction proceeds via formate, formyltetrahydrofolate (THF), and methenyl-, methylene-, and methyl-THF to a methylated acetyl coenzyme A (acetyl-CoA) synthase on which the methyl group is condensed with CO (derived from a second mol of CO_2) and CoA to acetyl-CoA (6–8). The subsequent conversion to acetate by the enzymes phosphotransacetylase and acetate kinase yields one ATP by substrate-level phosphorylation, but one ATP has to be reinvested for the synthesis of formyl-THF in the course of the formyl-THF synthetase reaction. Thus, the net ATP yield by substrate-level phosphorylation is zero (1). The problem of how this pathway is coupled to the synthesis of ATP has been solved recently in the acetogenic model organism *Acetobacterium woodii* (9, 10). In contrast to another model acetogen, *Moorella thermoacetica*, *A. woodii* does not have cytochromes (1, 11).

Acetogenesis from H_2 plus CO_2 in *A. woodii* is coupled to ATP synthesis by a chemiosmotic mechanism with Na^+ as the coupling ion (12). The Na^+ gradient is established by the Rnf complex, a membrane-bound enzyme complex composed of six subunits that harbors iron-sulfur centers as well as flavins and that catalyzes electron transfer from the low-potential donor reduced ferredoxin ($E_0' \approx -500$ mV) to NAD^+ ($E_0' = -320$ mV). This electron transfer reaction is coupled to vectorial Na^+ transport from the inner side to the outer side of the cell (9, 13). The electrochemical Na^+ gradient established across the cytoplasmic membrane is

Received 19 January 2015 **Accepted** 24 February 2015

Accepted manuscript posted online 2 March 2015

Citation Bertsch J, Öppinger C, Hess V, Langer JD, Müller V. 2015. Heterotrimeric NADH-oxidizing methylenetetrahydrofolate reductase from the acetogenic bacterium *Acetobacterium woodii*. J Bacteriol 197:1681–1689. doi:10.1128/JB.00048-15.

Editor: W. W. Metcalf

Address correspondence to Volker Müller, vmueller@bio.uni-frankfurt.de.

J.B. and C.Ö. contributed equally to this article.

Supplemental material for this article may be found at http://dx.doi.org/10.1128/JB.00048-15.

doi:10.1128/JB.00048-15

then used to drive ATP synthesis by a Na^+ F_1F_o ATP synthase (14, 15).

Since *A. woodii* has only the Rnf complex for energy conservation, the obvious issue is how ferredoxin is reduced. The redox potential of the ferredoxin in *A. woodii* can be considered to be in the range of ≈−500 mV; thus, electron transfer from hydrogen ($E_0' = -414$ mV) or NADH ($E_0' = -320$ mV) to ferredoxin is highly endergonic and thermodynamically unfavorable (16). Recently, electron bifurcation was discovered as a means of driving endergonic redox reactions by soluble enzyme complexes (17–20). The soluble hydrogenase from *A. woodii* is such an electron-bifurcating enzyme that drives the endergonic ferredoxin reduction with H_2 as the reductant by coupling it to the exergonic electron transfer from hydrogen to NAD^+ according to equation 1 (18):

$$2\ H_2 + Fd + NAD^+ \rightleftharpoons Fd^{2-} + NADH + 3\ H^+ \qquad (1)$$

Acetogens grow at the thermodynamic limit of life (16). Acetogenesis would allow the synthesis of only 0.3 mol ATP per mol acetate produced. Any reaction of the pathway that would yield additional reduced ferredoxin would increase the ATP yield significantly. The only reaction of the pathway that is exergonic enough is the reduction of methylene-THF to methyl-THF ($E_0' = -200$ mV) (21). With NADH as the reductant, the $\Delta G^{0'}$ is −23 kJ/mol, which is sufficient to drive ferredoxin reduction with NADH as the reductant by electron bifurcation, as recently suggested for *M. thermoacetica*. To address the issue of whether or not the MTHFR of *A. woodii* is electron bifurcating and coupled to ferredoxin reduction, we have purified the MTHFR from *A. woodii* and analyzed its enzymatic properties.

MATERIALS AND METHODS

Growth of cells and purification of the MTHFR of *A. woodii*. *A. woodii* (DSM 1030) was grown at 30°C under anoxic conditions in 20-liter flasks (Glasgerätebau Ochs, Germany) using 20 mM fructose to an optical density at 600 nm (OD_{600}) of ~2.5 as described previously (19). The medium and all buffers were prepared using the anaerobic techniques described previously (22, 23). All buffers used for preparation of cell extracts and purification contained 2 mM dithioerythritol (DTE) and 4 μM resazurin, and all purification steps were performed under strictly anaerobic conditions at room temperature in an anaerobic chamber (Coy Laboratory Products, USA) filled with 96% N_2 and 4% H_2. Cells of *A. woodii* were harvested and washed twice in 25 mM Tris buffer (pH 7) containing 420 mM saccharose. The cells were resuspended in 150 ml of 25 mM Tris buffer (pH 8) containing 420 mM saccharose and 500 mg lysozyme and incubated for 1 h at 37°C. After centrifugation, the protoplasts were resuspended in 25 mM Tris buffer (pH 7.6) containing 20 mM $MgSO_4$, 20% glycerol, 0.5 mM phenylmethylsulfonyl fluoride (PMSF), and 0.1 mg/ml DNase I and passed three times through a French pressure cell (110 MPa). Cell debris was removed by centrifugation at 24,000 × *g* for 40 min. Membranes were removed by centrifugation at 130,000 × *g* for 45 min. The supernatant containing the cytoplasmic fraction with approximately 2,573 mg protein was applied to a Q-Sepharose high-performance (HP) column equilibrated with buffer 1 (50 mM Tris-HCl, 20 mM $MgSO_4$, 20% glycerol, pH 7.6). Protein was eluted with a linear gradient of 180 ml from 0 mM to 300 mM NaCl in buffer 1. Methylene-THF-dependent NADH oxidation activity eluted at around 175 mM NaCl. Ammonium sulfate (1.2 M) was added to the pooled fractions, and these were loaded onto a phenyl-Sepharose HP column equilibrated with buffer 1 containing 1.2 M $(NH_4)_2SO_4$. Protein was eluted with a linear gradient of 200 ml from 1.2 to 0.6 M $(NH_4)_2SO_4$. Methylene-THF-dependent NADH oxidation activity eluted in a peak of around 1.0 M $(NH_4)_2SO_4$. Pooled fractions were concentrated using ultrafiltration in 100-kDa Vivaspin tubes (Sartorius Stedim Biotech GmbH, Germany). The concentrated sample was separated on a HiPrep Sephacryl S-300 HR column (16/60 GL; GE Healthcare) equilibrated with buffer 1. For the last purification step, using a HiTrap Blue-Sepharose HP column, the sample was applied to the column equilibrated with buffer 1. Protein was eluted with a stepwise elution with 0.5 M NaCl. The purified MTHFR was concentrated using ultrafiltration in 10-kDa Vivaspin tubes and stored at 4°C.

Enrichment of the protein that stimulates methyl-THF oxidation. For the enrichment of the protein(s) that stimulates methyl-THF oxidation, methyl-THF-dependent reduction of NAD^+ was determined in the presence of purified MTHFR. Cytoplasm of *A. woodii* was applied to a Q-Sepharose HP column equilibrated with buffer 1; the stimulating activity was found in the flowthrough. This sample was incubated at 60°C for 10 min, and denatured protein was removed by centrifugation. Ammonium sulfate was added to achieve a final concentration of 2 M, and the sample was applied to a phenyl-Sepharose HP column equilibrated with buffer 1 containing 2 M $(NH_4)_2SO_4$. The activity was eluted with a linear gradient of 150 ml from 2 to 0 M ammonium sulfate.

Enrichment of the methylene-THF dehydrogenase (MTHF-DH) of *A. woodii*. Cells were grown and harvested as described above. Cytoplasm of *A. woodii* was applied to a Q-Sepharose HP column equilibrated with buffer 1; MTHF-DH activity was found in the flowthrough. Ammonium sulfate (2 M) was added to the flowthrough and loaded onto a phenyl-Sepharose HP column equilibrated with buffer A containing 2 M $(NH_4)_2SO_4$. Protein was eluted with a linear gradient of 120 ml from 2 to 0 M $(NH_4)_2SO_4$. MTHF-DH activity eluted in a peak of around 1.0 M $(NH_4)_2SO_4$. Pooled fractions were concentrated using ultrafiltration in 10-kDa Vivaspin tubes. The concentrated sample was separated on a Superose 6 column (10/300 GL; GE Healthcare) followed by a Superdex 200 column (10/300 GL; GE Healthcare) using buffer A containing 100 mM NaCl for both runs. Next, the fractions containing MTHF-DH activity were incubated for 10 min at 60°C and denatured proteins were removed by centrifugation. The supernatant was applied to a Q-Sepharose HP column equilibrated with buffer 1 at pH 8.5. For the last purification step, the fractions containing MTHF-DH activity were pooled, desalted, and applied again to a Q-Sepharose HP column with buffer 1 at pH 8.5. The purified MTHF-DH was concentrated using ultrafiltration in 10-kDa Vivaspin tubes and stored at 4°C.

Heterologous expression of *metF* and *metVF*. Amplification of genes was done using Phusion DNA polymerase (New England BioLabs; Ipswitch, MA) and genomic DNA of *A. woodii* as the template. Primers used were as follows: for *metF*, 5′-ACGCGTCGACCGATTTTGCGATTGGTG CGATTCC-3′ (reverse) and 5′-AGTGCTAGCATGAGAATAACTGAGC TGTTTC-3′ (forward); for *metVF*, 5′-ATAGCTAGCATGTTGATTACC CAACTAAAATC-3′ (forward) and the reverse primer of *metF*. After amplification, the genes were cloned into the NheI and SalI sites of pET21a and transformed into *Escherichia coli* DH5α. Constructs were verified via DNA sequencing and introduced into *E. coli* C41(DE3), which already carried plasmids pRKISC (24) and pCodonPlus, for expression. For expression, cells were grown according to a previously described method (25). The cells were harvested, washed with lysis buffer A (50 mM NaH_2PO_4, 10 mM imidazole, 20% [vol/vol] glycerol, 300 mM NaCl, 10 μM [each] flavin mononucleotides [FMN], 2 mM DTE, pH 8), and used immediately for purification.

Purification of MetF-His and MetVF-His. All purification steps were performed under anoxic conditions. *E. coli* cells were disrupted via sonication in lysis buffer A. Cell debris was separated by centrifugation at 15,000 × *g* and 4°C for 30 min. The cell extract was incubated with 2 mM cysteine, 2.75 mM DTE, 0.5 mM $Fe(II)Cl_2$, 2 mM Na_2S, and 10 μM FMN for 4 h at 4°C with light stirring. Membranes and precipitated solids were removed by centrifugation at 120,000 × *g* for 90 min. The supernatant was diluted with anoxic lysis buffer B (50 mM NaH_2PO_4, 10 mM imidazole, 20% [vol/vol] glycerol, 300 mM NaCl, 10 μM FMN, pH 8) in a ratio of 1 to 5 and then loaded onto 5 ml nickel-nitrilotriacetic acid (Ni-NTA) material which was equilibrated with lysis buffer B. The column was

TABLE 1 Purification of the methylene-THF reductase of *A. woodii*

Purification step	Protein (mg)	MTHFR activity (μmol NADH/min per mg)[a]	Yield (%)	Purification (fold)
Cytoplasm	2,573	3.9	100	1
Q-Sepharose	166	53.3	88	13.9
Phenyl-Sepharose	42	178.3	75	46.6
Sephacryl S300	22	178.3	40	46.6
Blue-Sepharose	10	248	26	64.7

[a] MTHFR activity was measured by following the methylene-THF-dependent oxidation of NADH at 340 nm. The assay mixture contained 50 mM potassium phosphate buffer (pH 7), 2 mM DTE, 10 μM FMN, and 0.25 mM methylene-THF. All measurements were done under a gas atmosphere of 100% N_2 in anaerobic cuvettes at 30°C.

washed with washing buffer (50 mM NaH_2PO_4, 20 mM imidazole, 20% [vol/vol] glycerol, 300 mM NaCl, 10 μM FMN, pH 8). Recombinant protein was eluted with elution buffer (50 mM NaH_2PO_4, 150 mM imidazole, 20% [vol/vol] glycerol, 300 mM NaCl, 10 μM FMN, pH 8). Fractions containing the protein were pooled, concentrated, washed with storage buffer (50 mM NaH_2PO_4, 20% [vol/vol] glycerol, 300 mM NaCl, 10 μM FMN, pH 8), and stored at 4°C under nitrogen.

Enzymatic assays. All measurements (except the determination of the temperature optimum) were performed at 30°C in 1.8-ml anaerobic cuvettes (Glasgerätebau Ochs, Germany) sealed by rubber stoppers under a N_2 atmosphere. Methylene-THF was synthesized nonenzymatically with 0.5 mM THF (purchased from Sigma-Aldrich, Germany), 1.5 mM formaldehyde, and buffer 2 (50 mM potassium phosphate, 2 mM DTE, pH 7.0), leading to the formation of a racemic mixture (21, 26) and resulting in 0.25 mM "active" methylene-THF. Measurements were done routinely with a methylene-THF-dependent NADH oxidation assay with 0.25 mM NADH and 10 μM FMN by following the oxidation of NADH at 340 nm ($\varepsilon = 6.3\ mM^{-1}\ cm^{-1}$). For the determination of the temperature optimum, the enzyme was preincubated at the given temperature for 5 min. For the determination of the pH optimum, the measurements were carried out in buffer 3 {50 mM morpholineethanesulfonic acid (MES), 50 mM morpholinepropanesulfonic acid (MOPS), 50 mM Tris, 50 mM 2-(cyclohexylamino)ethanesulfonic acid (CHES), 50 mM 3-[(3-cholamidopropyl)-dimethylammonio]-1-propanesulfonate (CHAPS), 2 mM DTE, pH as indicated}. Ferredoxin was purified from *Clostridium pasteurianum* as described previously (27). When reduced ferredoxin (20 μM) or $FMNH_2$ (0.2 mM) was used as the electron donor, purified CO dehydrogenase–acetyl-CoA synthase (CODH/ACS) was used in a 100% CO atmosphere to reduce ferredoxin or FMN (10). For the measurement of the physiological reverse reaction, the methyl-THF-dependent reduction of NAD^+ (1 mM) was followed with 0.2 mM methyl-THF and 10 μM FMN in buffer 2. Heterologously produced MetF and MetVF were measured in buffer 2 with 50 μM FMN by following the methylene-THF-dependent oxidation of 10 mM methyl viologen (prereduced with sodium dithionite) at 604 nm ($\varepsilon = 13.8\ mM^{-1}\ cm^{-1}$). The activity of the MTHF-DH was measured by following the reduction of 1 mM NAD^+ at 340 nm in the presence of 0.25 mM methylene-THF in buffer 2.

Analytical methods. Protein concentration was measured according to the method of Bradford (28). Proteins were separated in 12% polyacrylamide gels and stained with Coomassie Brilliant Blue G250. The molecular mass of the purified methylene-THF reductase was determined by native gel electrophoresis. The proteins were identified by peptide mass fingerprinting. In brief, reduced and alkylated proteins were digested and analyzed using reversed-phase nano-high-performance liquid chromatography (nano-HPLC) (C_{18}, Proxeon easy-nLC) coupled to an electrospray ionization-quadrupole time of flight (ESI-q-TOF) mass spectrometer (Bruker maXis). Acquisition of mass spectra and fragmentation were based on the intensity and charge state of the precursor ions, and the mass lists were matched to a custom proteome database using the Mascot search engine (version 2.2.2; Matrix Sciences). When applicable, spectra were recalibrated using autoproteolytic fragments from trypsin and validated manually. The iron and sulfur content of the purified enzyme was determined by colorimetric methods (29). The flavin content was determined as described before (19).

For the determination of methyl-THF levels, protein was removed using ultrafiltration in 3-kDa Vivaspin tubes. The flowthrough was analyzed by HPLC on an Atlantis Silica HILIC column (Waters GmbH, Germany) (100 Å, 5 μm pore size, 2.1 mm by 15 mm) by using an isocratic elution with 33 mM potassium phosphate buffer (pH 3) containing 7% of acetonitrile at a flow rate of 1 ml/min. Methyl-THF was detected by measuring the absorbance at 351 nm.

RESULTS

Purification of the MTHFR of *A. woodii*. For the purification of the MTHFR, fructose-grown cells of *A. woodii* were harvested in the late-exponential-growth phase and disrupted in a French press. After low-speed centrifugation, the membrane fraction was removed by an ultracentrifugation step. Since the electron donors used for methylene-THF reduction are different in different organisms, we first determined whether the cytoplasmic fraction of *A. woodii* was able to use NADH as the reductant for methylene-THF reduction. Indeed, methylene-THF-dependent oxidation of NADH was observed, and this activity was used to follow the enzyme during its purification by four chromatographic steps on Q-Sepharose, phenyl-Sepharose, Sephacryl S-300, and Blue-Sepharose. Using this procedure, the enzyme was purified 65-fold with an average specific activity of 248 U/mg (Table 1).

When analyzed on a denaturing SDS gel, three proteins with molecular masses of 70, 31, and 23 kDa were visible. These masses are consistent with the masses predicted from the DNA sequences of RnfC2 (71.0 kDa), MetF (32.8 kDa), and MetV (22.7 kDa) (Fig. 1). The identities of the 70-, 31-, and 23-kDa proteins as RnfC2, MetF, and MetV, respectively, were finally confirmed by peptide mass fingerprinting. When the preparation was analyzed on a native gel, only one protein complex with an apparent molecular mass of 130 kDa (Fig. 2A) was visible. This is consistent with RnfC2, MetF, and MetV forming a stable complex of a heterotrimer with one copy of each subunit (calculated mass, 127 kDa).

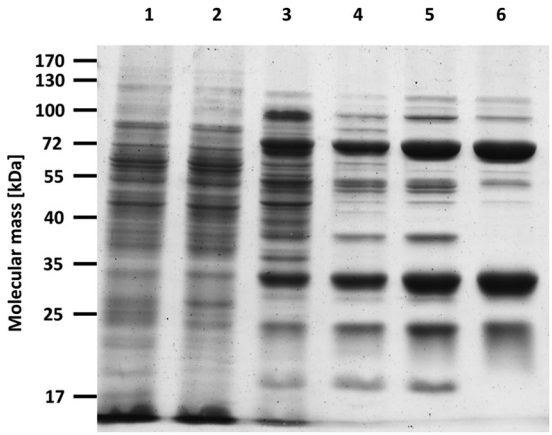

FIG 1 Purification of the methylene-THF reductase of *A. woodii*. Samples from the different purification steps were separated by SDS-PAGE, and proteins were stained with Coomassie Brilliant Blue. Lane 1, cell extract; lane 2, cytoplasm; lane 3, pooled fractions from Q-Sepharose; lane 4, pooled fractions from phenyl-Sepharose; lane 5, pooled fractions from Sephacryl S300; lane 6, pooled fractions from blue-Sepharose. A 10-μg volume of protein was applied to each lane.

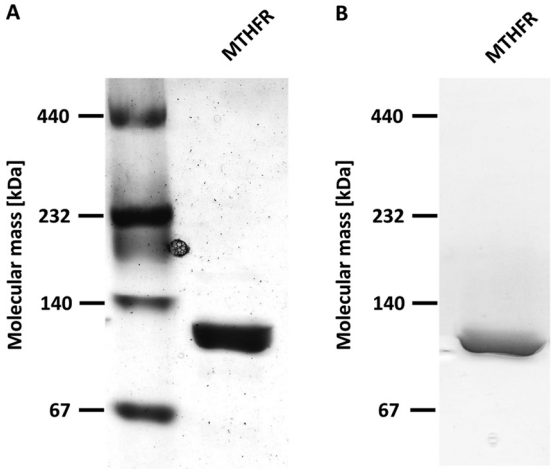

FIG 2 MetF, MetV, and RnfC2 build a stable methylene-THF reductase complex that catalyzes NADH:3-(4,5-dimethyl-2-thiazolyl)-2,5-diphenyl-2H-tetrazolium bromide (MTT) oxidoreductase activity. (A) The purified MTHFR (10 μg) was separated by native PAGE and stained with Coomassie Brilliant Blue. (B) NADH:MTT oxidoreductase activity was determined by incubation of the gel in 10 mM KH_2PO_4 (pH 7.5) with MTT tetrazolium dye and NADH.

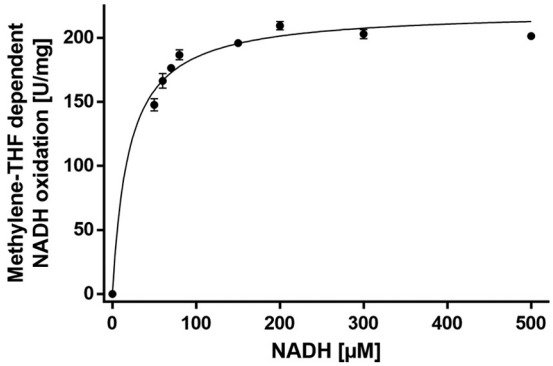

FIG 4 NADH dependence of methylene-THF reductase activity. The methylene-THF-dependent oxidation of NADH was measured in 50 mM potassium phosphate buffer (pH 7) containing 2 mM DTE and 0.25 mM methylene-THF with 10 μM FMN and various amounts of NADH. The activity followed Michaelis-Menten kinetics with a V_{max} (maximal enzyme velocity) of 212 U/mg and a K_m (Michaelis constant) of 19 μM. Curve fitting and determination of the kinetic parameters K_m and V_{max} were performed using the GraphPad Prism program (version 4.03) and the Michaelis-Menten equation [$Y = (V_{max} \times X)/(K_m + X)$].

This complex also catalyzed NADH:methyltetrazolium chloride oxidoreductase activity in a native gel (Fig. 2B).

Basic biochemical properties of the MTHFR of *A. woodii*. So far, most purified MTHFRs have contained non-covalently bound flavin adenine dinucleotide (FAD) as an essential cofactor (26, 30–34). An exception is the MTHFR from *M. thermoacetica* that contains FMN (25). When the MTHFR of *A. woodii* was purified in the absence of flavins, a peak around 380 nm was observed in the UV light-visible light spectrum (Fig. 3), which is typical for the presence of flavins (35). After release of the flavin from the enzyme by precipitation with trichloroacetic acid and subsequent separation of the supernatant by thin-layer chromatography, the flavin was identified as FMN, which is consistent with the MTHFR from *Moorella thermoacetica* (25) but in contrast to most known MTHFRs, which instead contain FAD. In sum, a value of 1.9 mol FMN/mol MTHFR was calculated, which is in agreement with the presence of a flavin binding site in each of MetF and RnfC2. Furthermore, the purified MTHFR from *A. woodii* contained 23.5 ± 1.2 mol of iron/mol of protein and 24.5 ± 1.5 mol sulfur/mol of protein, which fits well with the predicted two [4Fe4S] clusters in MetV and four [4Fe4S] clusters in RnfC2.

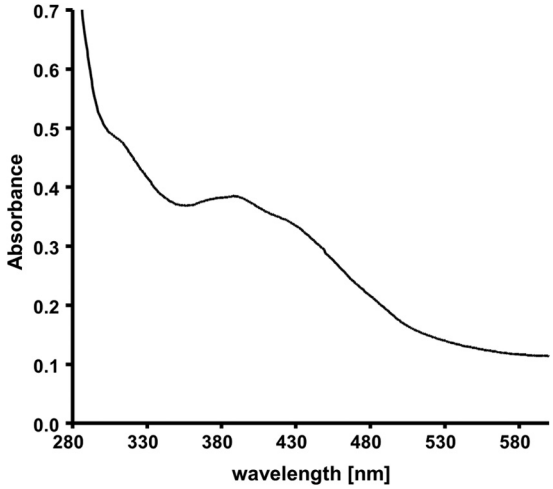

FIG 3 UV light/visible light spectrum of the purified methylene-THF reductase. The spectrum of the enzyme (0.6 mg/ml) was recorded in 50 mM potassium phosphate buffer (pH 7) containing 2 mM DTE.

The oxidation of NADH with methylene-THF as the electron acceptor was used to determine the basic properties of the purified enzyme. The MTHFR had a rather broad temperature range (10 to 60°C) for activity, whereas the maximum activity was observed at 30°C, the optimal growth temperature of *A. woodii*. The pH optimum was at pH 7.0 and decreased to ~60% at pH 5.5 or 8.0. The presence of ions such as Na^+, K^+, Mg^{2+}, Ca^{2+}, Cl^-, and SO_4^{2-} (50 mM each) had no effect on activity. Besides the NADH:methylene-THF-reductase activity, the purified enzyme also catalyzed the reduction of potassium ferricyanide (36 U/mg), methyl viologen (300 U/mg), and FMN (1.9 U/mg) with NADH as the electron donor.

The physiological reaction catalyzed by the MTHFR of *A. woodii*. The purified enzyme could oxidize NADH in the presence of methylene-THF. This is in sharp contrast to the MTHFR purified recently from *M. thermoacetica* (25). Seven hundred picomoles of NADH was oxidized by 1 pmol enzyme (in the absence of added FMN), indicating that the observed electron flow was not only to enzyme-bound FMN but was further to the acceptor. Indeed, methyl-THF formation was observed and the stoichiometry was 1:1 (NADH:methyl-THF).

When ferredoxin (reduced by purified CODH/ACS in a 100% CO atmosphere) was used as the electron donor, formation of methyl-THF was observed but at only a very low rate; the amount of methyl-THF after 20 min was the same as with NADH after 20 s. NADPH was not used as the electron donor. These data are consistent with the hypothesis that NADH is the physiological electron donor but that ferredoxin may also be used under certain physiological conditions. The dependence of the reaction on NADH followed Michaelis-Menten kinetics, with saturation at 200 μM and an apparent K_m of 19 ± 2 μM (Fig. 4). When FMN (5

μM) was added, the oxidation of NADH (with reduction of methylene-THF) was stimulated ~2- to ~4-fold, whereas the addition of FAD did not stimulate this activity. Maximum activity was observed with 2 μM FMN, indicating the role of FMN as a cofactor.

The reduction of methylene-THF with NADH is an exergonic reaction, and it has been proposed that this exergonic redox reaction might drive the reduction of ferredoxin with NADH via flavin-based electron bifurcation (3, 36). Therefore, we analyzed the reaction for ferredoxin dependence or stimulation. All other known electron-bifurcating enzymes that drive endergonic ferredoxin reduction are strictly coupled; i.e., no or only little activity could be observed in the absence of ferredoxin (or of the second electron acceptor) (17–20, 37–44). In contrast, the NADH-dependent reduction of methylene-THF catalyzed by the MTHFR of *A. woodii* was independent of ferredoxin. In the absence of ferredoxin, the activity was already 248 U/mg, which is in the same range as the MTHF-DH (45). The enzymatic activity could not be stimulated by addition of oxidized ferredoxin, and reduction of ferredoxin was never observed. With all the conditions tested, we could not find any indications for a ferredoxin-reducing electron-bifurcating MTHFR in *A. woodii*.

Reactions catalyzed by heterologously produced MetF and MetVF. To analyze the role of the single subunits in the complex, *metF* and *metV*, together with *metF*, were individually cloned into an expression vector, expressed in *E. coli*, and purified via affinity chromatography. The MTHFR complex purified from *A. woodii* catalyzed the electron transfer from NADH to methylene-THF. MetF alone could not catalyze this reaction, even when NADH was replaced by reduced viologen dyes. Since MetV stimulates the activity of MetF (25), MetV was purified together with MetF. MetVF also could not catalyze the methylene-THF-dependent oxidation of NADH. However, MetVF oxidized reduced methyl viologen with methylene-THF as the electron acceptor with a specific activity of 33 mU/mg. Thus, MetVF was able to reduce methylene-THF, and hence seems to be the entry point for electrons coming from methyl viologen, but was unable to oxidize NADH. Consequently, the third subunit RnfC2 has to be the entry point for electrons derived from NADH. This hypothesis is supported by the results of bioinformatic analyzes showing that RnfC2 contains a putative NADH binding site whereas the supposed NADH binding site in MetF is altered (see Discussion).

Oxidation of methyl-THF is not mechanistically blocked. Thermodynamically, oxidation of methyl-THF with reduction of NAD^+ is highly endergonic and the reaction could not be observed with the purified protein. As stated above, the MTHFR of *A. woodii* can reduce methyl viologen and FMN with NADH as the electron donor. These reactions were reversible, and NAD^+ was reduced with reduced methyl viologen as the donor (150 U/mg). However, when $FMNH_2$ was the electron donor, the specific activity was only 50 mU/mg, which is only 2% of the level seen with the forward reaction. When methyl-THF was used as the electron donor, NAD^+ reduction was never observed. Despite several attempts, we were not able to drive NAD^+-dependent methyl-THF oxidation by addition of reduced ferredoxin. This is consistent with the statement that the MTHFR is not electron bifurcating. In contrast, the cytoplasmic fraction of *A. woodii* was able to reduce NAD^+ upon addition of methyl-THF, demonstrating that the enzyme can catalyze the backward reaction and is not blocked mechanistically. Addition of an aliquot of cell extract to the purified MTHFR stimulated NAD^+ reduction coupled to methyl-THF oxidation, but this stimulation was no longer detected when the cell extract was boiled (80°C for 10 min), indicating that the stimulating factor was a protein. Cell extract was then fractionated, and the fractions were analyzed for stimulation of the NAD^+-dependent methyl-THF oxidation by the purified MTHFR (see Table S1 in the supplemental material). This yielded a proteinaceous fraction with high methylene-THF dehydrogenase (MTHF-DH) activity. The MTHF-DH was then enriched by classical chromatography from a cell extract; this preparation had a MTHF-DH activity of 1,200 U/mg (see Table S2) and contained a major protein of 33 kDa, corresponding to the predicted molecular mass of the MTHF-DH (see Fig. S1 in the supplemental material). The sample was not able to reduce NAD^+ in the presence of methyl-THF, but in combination with the purified MTHFR, the reduction of NAD^+ was observed (Fig. 5). These data demonstrate that the enzyme is not mechanistically impaired in oxidation of methyl-THF. As expected from the thermodynamics, the reaction is "pulled" by removal of the product methylene-THF.

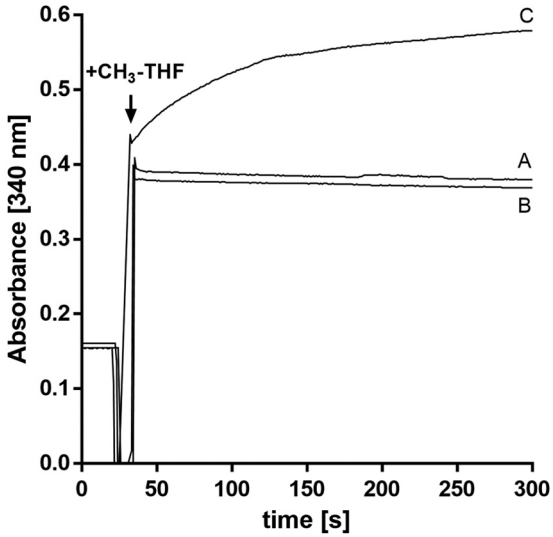

FIG 5 A second protein is required for MTHFR-catalyzed oxidation of methyl-THF. The methyl-THF-dependent reduction of NAD^+ was measured in 50 mM potassium phosphate buffer (pH 7) containing 2 mM DTE, 1 mM NAD^+, 10 μM FMN, and 0.2 mM methyl-THF in the presence of the purified MTHFR (13 μg) (A), the sample containing the enriched MTHF-DH (0.75 μg) (B), or the MTHFR and the enriched MTHF-DH (C). CH_3-THF, methyl-THF.

DISCUSSION

Genomic organization of the MTHFR of *A. woodii*. From the genetic data, the MTHFR is postulated to have three subunits, encoded by Awo_c09290 to Awo_c09310, that are part of the cluster of the genes that encode the enzymes catalyzing the reduction of formyl-THF to methyl-THF. Awo_c09290 to Awo_c09310 are cotranscribed, indicating that the gene products are in a functional context (3). *metF* encodes the predicted large subunit of the MTHFR with a conserved flavin binding site, *metV* the small subunit of the reductase, and *rnfC2* a hitherto-unknown subunit of a MTHFR complex.

Modularity of the MTHFR from different species. The simplest form of the MTHFR consists solely of MetF, which catalyzes the irreversible reduction of methylene-THF with NADH. Classical examples of those modules are the MTHFRs from *E. coli* and

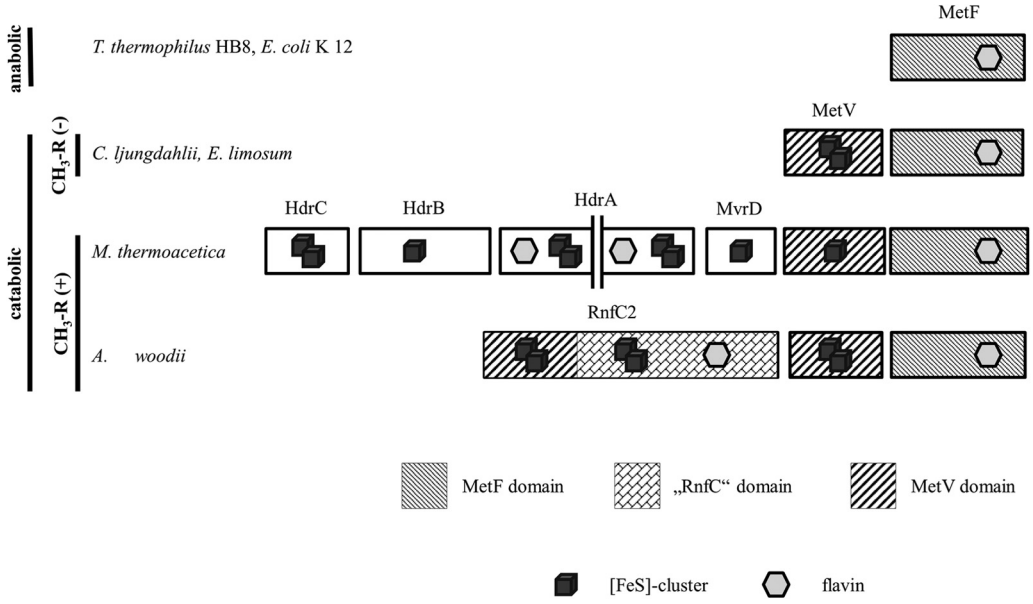

FIG 6 Genetic organization of methylene-THF reductase complexes. Hdr, heterodisulfide reductase; Mvh, methyl viologen reducing hydrogenase; anabolic/catabolic, physiological roles of the MTHFR in the corresponding organism; CH_3-R(+), the organisms are reported to grow on methylated substrates; CH_3-R(-), the organisms are not reported to grow on methylated substrates.

Thermus thermophilus HB8 (Fig. 6). Crystal structures of the enzymes from *E. coli* and *T. thermophilus* HB8 (34, 46) suggest a shared binding site for NAD(P)H and methylene-THF near the FAD flavin cofactor. NAD(P)H reduces the flavin to FADH, and the residual $NAD(P)^+$ exits the binding pocket to make way for methylene-THF, which in turn gets reduced by the enzyme-bound FADH. MetF of *A. woodii* is 37% identical to MetF from *M. thermoacetica* and 44% identical to MetF from *Eubacterium limosum*. MetF from *Clostridium ljungdahlii* is even 49% identical to MetF from *A. woodii*. None of these MetFs has a predicted NADH binding site, and other proteins are involved (see next paragraph). On the other hand, MetF from *E. coli* shows merely a sequence identity of approximately 22% to 23% to the acetogenic MetF subunits.

In acetogenic bacteria, the MTHFR is part of the catabolic route and enzymatic activities should be much higher than those seen with MetF from, for example, *E. coli*. Indeed, the additional MetV subunit has been shown to stimulate methylene-THF reduction catalyzed by MetF dramatically (25). MetV is predicted to have bound Zn^{2+} ions and to contain iron-sulfur clusters. The purified MTHFR from *Clostridium formicoaceticum* had a $\alpha_4\beta_4$ composition of subunits with molecular masses of 35 and 26 kDa, presumably representing MetF and MetV. Interestingly, the electron donor for the reduction of methylene-THF was not NAD(P)H but reduced ferredoxin (31). The enzyme contains iron, acid-labile sulfur, and FAD, whereas the *E. coli* MetF—a 33-kDa protein—has only FAD. Therefore, one might suggest that MetV augments MetF to use reduced ferredoxin to catalyze the reaction from methylene-THF to methyl-THF, which fits our results showing that reduced ferredoxin also led to formation of methyl-THF. Unfortunately, no genetic data are available to investigate the genomic distribution of *metV* and *metF* in *C. formicoaceticum*. In contrast, the acetogen *Clostridium autoethanogenum* also has MetVF, which oxidizes neither NAD(P)H nor reduced ferredoxin (41). The use of ferredoxin as the reductant by MetVF may be artificial, and the "*in vivo*" electron donor may be a flavodoxin or thioredoxin with a redox potential in the same range as NADH. The small subunit of the MTHFR from *A. woodii* MetV shows comparatively high sequence similarities of 35% to 37% to the corresponding MetV proteins from *C. ljungdahlii*, *M. thermoacetica*, and *E. limosum*.

In some organisms, there is a third module in addition to MetVF. A MTHFR preparation from *M. thermoacetica* contained, besides MetVF, the heterodisulfide reductase subunits HdrABC and MvrD, along with other proteins (25). The complex could reduce methylene-THF with benzyl viologen as the donor and oxidize NADH with benzyl viologen as the acceptor. Experiments with heterologously produced subunits demonstrated that MetF is the site of methylene-THF reduction and HdrA the site of NADH oxidation. But, in contrast to the MTHFR of *A. woodii*, the complex of *M. thermoacetica* was not able to catalyze the methylene-THF-dependent oxidation of NADH. Since an involvement of ferredoxin could not be confirmed, those authors speculated that the MTHFR of *M. thermoacetica* conveys electron bifurcation from NADH to methylene-THF and a so-far-unknown second acceptor. This hypothesis is strengthened by the fact that known electron-bifurcating enzymes are strictly coupled; i.e., even the energetic downhill reaction is not catalyzed in the absence of the second electron acceptor.

The MTHFR purified from *A. woodii* shows a novel modularity. It is built by subunits MetF, MetV, and RnfC2, most likely in a 1:1:1 stoichiometry (Fig. 7). The C terminus of RnfC2 is 41% identical to the RnfC subunit of the Rnf complex, and both have a putative NADH binding site (see Fig. S2 in the supplemental material) (47). In addition, RnfC2 has a putative flavin binding site. Of the two Fe/S binding sites with the consensus sequence $CX_2CX_2CX_3CP$, one is completely conserved and only the last proline is changed, to a serine, in the second. Additionally, RnfC2 contains

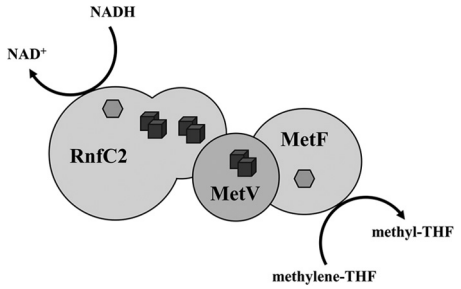

FIG 7 Model of the methylene-THF reductase complex of *A. woodii*. Hexagons represent flavins; cubes represent iron-sulfur clusters.

an N-terminal extension of 220 amino acids with 40% identity to MetV. In this extension, the 8 cysteine residues for a potential coordination of two iron-sulfur clusters are also conserved. Thus, RnfC2 is a fusion of RnfC and MetV. Accordingly, it can be surmised that RnfC2 contains four iron-sulfur clusters and a FMN and conveys the ability to oxidize NADH to the enzyme. All the data obtained here are consistent with the hypothesis that the MTHFR from *A. woodii* does not use electron bifurcation to couple the exergonic electron transfer from NADH to methylene-THF to an endergonic redox reaction.

The striking modularity of the MTHFRs in different organisms and the differential biological activities may suggest an evolutionary line for MTHFRs (Fig. 6). Enzymes containing only MetF allow cells to reduce methylene-THF with NAD(P)H. In these organisms, the reaction is purely anabolic. Addition of MetV may lead to two achievements: an additional entry point for electrons, i.e., from ferredoxin or flavodoxin, and, most important, an increase of the methylene-THF reduction rate to the values necessary for catabolic enzymes. Addition of the third module must have gone along with a change in the reaction mechanism in MetF since the electrons are now donated via the third module. This scenario is consistent with the fact that MetF of *A. woodii* and *M. thermoacetica* lost the ability to bind and oxidize NADH. This is supported by an amino acid change in acetogenic MetF subunits that have methionine in place of phenylalanine, which has a crucial role in *E. coli* MTHFR for NADH binding (48). Addition of the third module also gives the cell some more flexibility for energetics and interaction. The Hdr module in *M. thermoacetica* is suggested to introduce an electron-bifurcating pathway into the MTHFR, but this is not observed in *A. woodii*. RnfC2 of *A. woodii* may allow the MTHFR to interact directly with the membrane-bound Rnf complex (3).

The role of the MTHFR during growth on methylated substrates. The third module may also allow circumvention of a serious energetic barrier. Both *A. woodii* and *M. thermoacetica* are known to grow on methylated substrates (49, 50), which is in contrast to results seen with *C. ljungdahlii* and *E. limosum*. The methyl group of methylated substrates is transferred to THF, yielding methyl-THF (51), which has to be oxidized to CO_2 in order to generate the reducing equivalents for reduction of CO_2 to CO. However, the first step in oxidation, methyl-THF to methylene-THF, is highly endergonic ($\Delta G^{0\prime} = +23$ kJ/mol [52])—so endergonic that, in organisms such as *E. coli* or eukaryotes, the methyl group is trapped as methyl-THF and can be released only by demethylation and not by oxidation. But acetogens growing on methyl groups containing substrates somehow have to oxidize methyl-THF. The high energy barrier for NAD-dependent meth-

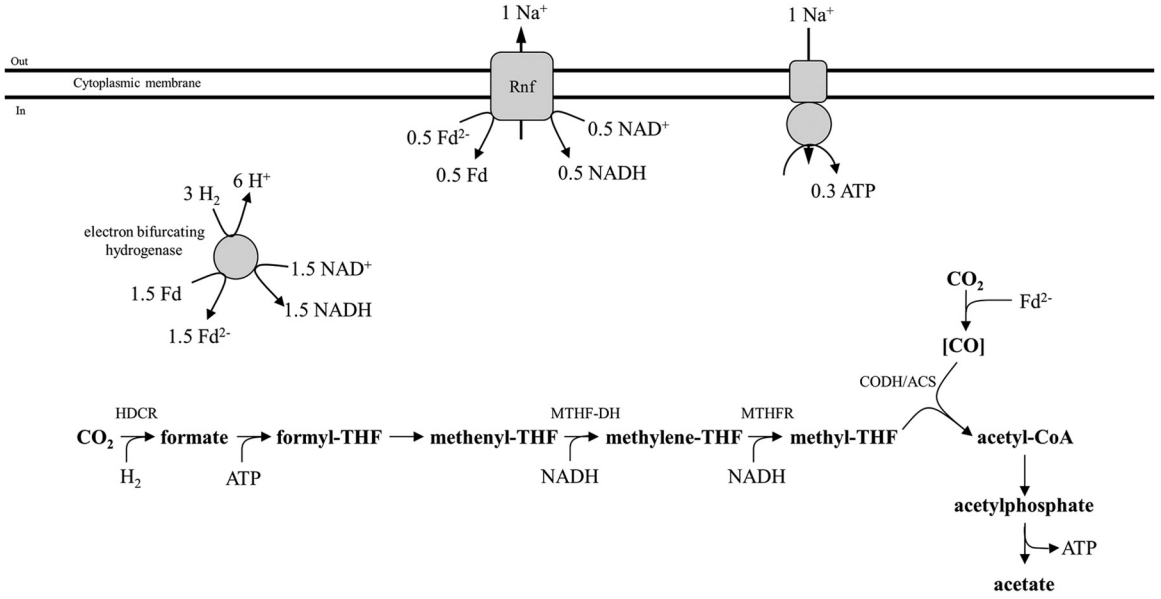

$$4\ H_2 + 2\ CO_2 \rightarrow 1\ acetate^- + 1\ H^+ + 2\ H_2O \quad \Delta G^{0\prime} = -95\ kJ/mol$$
$$0.3\ ATP/acetate$$

FIG 8 Bioenergetics of acetogenesis from H_2 plus CO_2 in *A. woodii*. For explanations, see the text. HDCR, H_2-dependent CO_2 reductase.

yl-THF oxidation could be overcome by a reversal of electron bifurcation—electron confurcation. Examples are the hydrogen-evolving hydrogenase of *Thermotoga maritima* (37) and the lactate dehydrogenase of *A. woodii* (44). Both enzymes use reduced ferredoxin as the coreductant and the driving force for an endergonic redox reaction. Also, the Hdr-containing MTHFR from *M. thermoacetica* may use electron bifurcation to drive methyl-THF oxidation with NAD^+ as the oxidant (25). Apparently, methyl-THF oxidation in *A. woodii* could not be driven by oxidation of reduced ferredoxin. In contrast, methyl-THF-dependent NAD^+ reduction was observed after addition of a MTHF-DH-containing protein fraction. This shows that, in principle, the reaction of the MTHFR is reversible and the enzyme can catalyze the first oxidation step. One possible explanation for these findings would be that the NAD^+-dependent MTHF-DH removes the product of the MTHFR by oxidizing methylene-THF to methenyl-THF and therefore pulls the reaction toward NAD^+ reduction.

Energetics of acetate formation from H_2 plus CO_2 in *A. woodii*. The MTHFR of *A. woodii* was the last piece of the puzzle of the bioenergetics in *A. woodii*. It is apparently not electron bifurcating and thus is not involved in energy conservation. However, we cannot currently exclude the possibility that, under certain growth conditions, the MTHFR is the electron acceptor of the Rnf complex via RnfC2 (3). If this were true, Fd-dependent methylene-THF reduction would lead to Na^+ translocation. However, ferredoxin-dependent reduction of NAD^+ or methylene-THF would lead to the same amount of Na^+ translocated. Apparently, the electron-bifurcating hydrogenase of *A. woodii* (18) is the only source for ferredoxin reduction. CO_2 reduction to formate, catalyzed by the H_2-dependent CO_2 reductase (53), requires molecular hydrogen. Since the two subsequent reduction steps require NADH and the reduction of CO_2 to CO requires reduced ferredoxin, only 0.5 mol of reduced ferredoxin is left to fuel the Rnf complex. With a Na^+/ATP stoichiometry of 3.3 (54), this yields only 0.3 mol ATP per mol of acetate produced (Fig. 8).

ACKNOWLEDGMENTS

Financial support by the Deutsche Forschungsgemeinschaft (V.M.), the Deutsche Bundesstiftung Umwelt (J.B.), and the ESFRI-Instruct program of the European Union (J.D.L.) is gratefully acknowledged.

We are indebted to E. Trimmer, Grinnell College, for valuable discussion. We thank R. K. Thauer for supplying cells of *E. coli* C41(DE3).

REFERENCES

1. **Müller V.** 2003. Energy conservation in acetogenic bacteria. Appl Environ Microbiol **69:**6345–6353. http://dx.doi.org/10.1128/AEM.69.11.6345-6353.2003.
2. **Drake HL, Daniel S, Küsel K, Matthies C, Kuhner C, Braus-Strohmeyer S.** 1997. Acetogenic bacteria: what are the in situ consequences of their diverse metabolic diversities? BioFactors **6:**13–24. http://dx.doi.org/10.1002/biof.5520060103.
3. **Poehlein A, Schmidt S, Kaster A-K, Goenrich M, Vollmers J, Thürmer A, Bertsch J, Schuchmann K, Voigt B, Hecker M, Daniel R, Thauer RK, Gottschalk G, Müller V.** 2012. An ancient pathway combining carbon dioxide fixation with the generation and utilization of a sodium ion gradient for ATP synthesis. PLoS One **7:**e33439. http://dx.doi.org/10.1371/journal.pone.0033439.
4. **Berg IA, Kockelkorn D, Ramos-Vera WH, Say RF, Zarzycki J, Hugler M, Alber BE, Fuchs G.** 2010. Autotrophic carbon fixation in archaea. Nat Rev Microbiol **8:**447–460. http://dx.doi.org/10.1038/nrmicro2365.
5. **Ragsdale SW, Pierce E.** 2008. Acetogenesis and the Wood-Ljungdahl pathway of CO_2 fixation. Biochim Biophys Acta **1784:**1873–1898. http://dx.doi.org/10.1016/j.bbapap.2008.08.012.
6. **Ragsdale SW.** 2008. Enzymology of the Wood-Ljungdahl pathway of acetogenesis. Ann N Y Acad Sci **1125:**129–136. http://dx.doi.org/10.1196/annals.1419.015.
7. **Ljungdahl LG.** 1994. The acetyl-CoA pathway and the chemiosmotic generation of ATP during acetogenesis, p 63–87. *In* Drake HL (ed), Acetogenesis. Chapman & Hall, New York, NY.
8. **Wood HG, Ragsdale SW, Pezacka E.** 1986. The acetyl-CoA pathway of autotrophic growth. FEMS Microbiol Rev **39:**345–362. http://dx.doi.org/10.1111/j.1574-6968.1986.tb01865.x.
9. **Biegel E, Schmidt S, González JM, Müller V.** 2011. Biochemistry, evolution and physiological function of the Rnf complex, a novel ion-motive electron transport complex in prokaryotes. Cell Mol Life Sci **68:**613–634. http://dx.doi.org/10.1007/s00018-010-0555-8.
10. **Hess V, Schuchmann K, Müller V.** 2013. The ferredoxin:NAD^+ oxidoreductase (Rnf) from the acetogen *Acetobacterium woodii* requires Na^+ and is reversibly coupled to the membrane potential. J Biol Chem **288:**31496–31502. http://dx.doi.org/10.1074/jbc.M113.510255.
11. **Balch WE, Schoberth S, Tanner RS, Wolfe RS.** 1977. *Acetobacterium*, a new genus of hydrogen-oxidizing, carbon-dioxide-reducing, anaerobic bacteria. Int J Syst Bact **27:**355–361. http://dx.doi.org/10.1099/00207713-27-4-355.
12. **Imkamp F, Müller V.** 2002. Chemiosmotic energy conservation with Na^+ as the coupling ion during hydrogen-dependent caffeate reduction by *Acetobacterium woodii*. J Bacteriol **184:**1947–1951. http://dx.doi.org/10.1128/JB.184.7.1947-1951.2002.
13. **Biegel E, Müller V.** 2010. Bacterial Na^+-translocating ferredoxin:NAD^+ oxidoreductase. Proc Natl Acad Sci U S A **107:**18138–18142. http://dx.doi.org/10.1073/pnas.1010318107.
14. **Heise R, Müller V, Gottschalk G.** 1992. Presence of a sodium-translocating ATPase in membrane vesicles of the homoacetogenic bacterium *Acetobacterium woodii*. Eur J Biochem **206:**553–557. http://dx.doi.org/10.1111/j.1432-1033.1992.tb16959.x.
15. **Fritz M, Müller V.** 2007. An intermediate step in the evolution of ATPases—the F_1F_o-ATPase from *Acetobacterium woodii* contains F-type and V-type rotor subunits and is capable of ATP synthesis. FEBS J **274:**3421–3428. http://dx.doi.org/10.1111/j.1742-4658.2007.05874.x.
16. **Schuchmann K, Müller V.** 2014. Autotrophy at the thermodynamic limit of life: a model for energy conservation in acetogenic bacteria. Nat Rev Microbiol **12:**809–821. http://dx.doi.org/10.1038/nrmicro3365.
17. **Li F, Hinderberger J, Seedorf H, Zhang J, Buckel W, Thauer RK.** 2008. Coupled ferredoxin and crotonyl coenzyme A (CoA) reduction with NADH catalyzed by the butyryl-CoA dehydrogenase/Etf complex from *Clostridium kluyveri*. J Bacteriol **190:**843–850. http://dx.doi.org/10.1128/JB.01417-07.
18. **Schuchmann K, Müller V.** 2012. A bacterial electron bifurcating hydrogenase. J Biol Chem **287:**31165–31171. http://dx.doi.org/10.1074/jbc.M112.395038.
19. **Bertsch J, Parthasarathy A, Buckel W, Müller V.** 2013. An electron-bifurcating caffeyl-CoA reductase. J Biol Chem **288:**11304–11311. http://dx.doi.org/10.1074/jbc.M112.444919.
20. **Buckel W, Thauer RK.** 2013. Energy conservation via electron bifurcating ferredoxin reduction and proton/Na^+ translocating ferredoxin oxidation. Biochim Biophys Acta **1827:**94–113. http://dx.doi.org/10.1016/j.bbabio.2012.07.002.
21. **Wohlfarth G, Diekert G.** 1991. Thermodynamics of methylenetetrahydrofolate reduction to methyltetrahydrofolate and its implications for the energy metabolism of homoacetogenic bacteria. Arch Microbiol **155:**378–381. http://dx.doi.org/10.1007/BF00243458.
22. **Hungate RE.** 1969. A roll tube method for cultivation of strict anaerobes, p 117–132. *In* Norris JR, Ribbons DW (ed), Methods in microbiology, vol 3b. Academic Press, New York, NY.
23. **Bryant MP.** 1972. Commentary on the Hungate technique for culture of anaerobic bacteria. Am J Clin Nutr **25:**1324–1328.
24. **Takahashi Y, Nakamura M.** 1999. Functional assignment of the ORF2-*iscS-iscU-iscA-hscB-hscA-fdx*-ORF3 gene cluster involved in the assembly of Fe-S clusters in *Escherichia coli*. J Biochem **126:**917–926. http://dx.doi.org/10.1093/oxfordjournals.jbchem.a022535.
25. **Mock J, Wang S, Huang H, Kahnt J, Thauer RK.** 2014. Evidence for a hexaheteromeric methylenetetrahydrofolate reductase in *Moorella thermoacetica*. J Bacteriol **196:**3303–3314. http://dx.doi.org/10.1128/JB.01839-14.
26. **Sheppard CA, Trimmer EE, Matthews RG.** 1999. Purification and properties of NADH-dependent 5, 10-methylenetetrahydrofolate reductase (MetF) from *Escherichia coli*. J Bacteriol **181:**718–725.

27. **Schönheit P, Wäscher C, Thauer RK.** 1978. A rapid procedure for the purification of ferredoxin from clostridia using polyethylenimine. FEBS Lett **89:**219–222. http://dx.doi.org/10.1016/0014-5793(78)80221-X.
28. **Bradford MM.** 1976. A rapid and sensitive method for the quantitation of microgram quantities of protein utilizing the principle of protein-dye binding. Anal Biochem **72:**248–254. http://dx.doi.org/10.1016/0003-2697(76)90527-3.
29. **Fish WW.** 1988. Rapid colorimetric micromethod for the quantitation of complexed iron in biological samples. Methods Enzymol **158:**357–364. http://dx.doi.org/10.1016/0076-6879(88)58067-9.
30. **Daubner SC, Matthews RG.** 1982. Purification and properties of methylenetetrahydrofolate reductase from pig liver. J Biol Chem **257:**140–455.
31. **Clark JE, Ljungdahl LG.** 1984. Purification and properties of 5,10-methylenetetrahydrofolate reductase, an iron-sulfur flavoprotein from *Clostridium formicoaceticum*. J Biol Chem **259:**10845–10849.
32. **Wohlfarth G, Geerligs G, Diekert G.** 1990. Purification and properties of a NADH-dependent 5,10-methylenetetrahydrofolate reductase from *Peptostreptococcus productus*. Eur J Biochem **192:**411–417. http://dx.doi.org/10.1111/j.1432-1033.1990.tb19242.x.
33. **Zhou J, Kang SS, Wong PW, Fournier B, Rozen R.** 1990. Purification and characterization of methylenetetrahydrofolate reductase from human cadaver liver. Biochem Med Metab Biol **43:**234–242. http://dx.doi.org/10.1016/0885-4505(90)90029-Z.
34. **Igari S, Ohtaki A, Yamanaka Y, Sato Y, Yohda M, Odaka M, Noguchi K, Yamada K.** 2011. Properties and crystal structure of methylenetetrahydrofolate reductase from *Thermus thermophilus* HB8. PLoS One **6:**e23716. http://dx.doi.org/10.1371/journal.pone.0023716.
35. **Hetzel M, Brock M, Selmer T, Pierik AJ, Golding BT, Buckel W.** 2003. Acryloyl-CoA reductase from *Clostridium propionicum*. An enzyme complex of propionyl-CoA dehydrogenase and electron-transferring flavoprotein. Eur J Biochem **270:**902–910.
36. **Köpke M, Held C, Hujer S, Liesegang H, Wiezer A, Wollherr A, Ehrenreich A, Liebl W, Gottschalk G, Dürre P.** 2010. *Clostridium ljungdahlii* represents a microbial production platform based on syngas. Proc Natl Acad Sci U S A **107:**13087–13092. http://dx.doi.org/10.1073/pnas.1004716107.
37. **Schut GJ, Adams MW.** 2009. The iron-hydrogenase of *Thermotoga maritima* utilizes ferredoxin and NADH synergistically: a new perspective on anaerobic hydrogen production. J Bacteriol **191:**4451–4457. http://dx.doi.org/10.1128/JB.01582-08.
38. **Wang S, Huang H, Moll J, Thauer RK.** 2010. $NADP^+$ reduction with reduced ferredoxin and $NADP^+$ reduction with NADH are coupled *via* an electron bifurcating enzyme complex in *Clostridium kluyveri*. J Bacteriol **192:**5115–5123. http://dx.doi.org/10.1128/JB.00612-10.
39. **Kaster AK, Moll J, Parey K, Thauer RK.** 2011. Coupling of ferredoxin and heterodisulfide reduction via electron bifurcation in hydrogenotrophic methanogenic archaea. Proc Natl Acad Sci U S A **108:**2981–2986. http://dx.doi.org/10.1073/pnas.1016761108.
40. **Huang H, Wang S, Moll J, Thauer RK.** 2012. Electron bifurcation involved in the energy metabolism of the acetogenic bacterium *Moorella thermoacetica* growing on glucose or H_2 plus CO_2. J Bacteriol **194:**3689–3699. http://dx.doi.org/10.1128/JB.00385-12.
41. **Wang S, Huang H, Kahnt J, Mueller AP, Köpke M, Thauer RK.** 2013. NADP-specific electron-bifurcating [FeFe]-hydrogenase in a functional complex with formate dehydrogenase in *Clostridium autoethanogenum* grown on CO. J Bacteriol **195:**4373–4386. http://dx.doi.org/10.1128/JB.00678-13.
42. **Wang S, Huang H, Kahnt J, Thauer RK.** 2013. *Clostridium acidurici* electron-bifurcating formate dehydrogenase. Appl Environ Microbiol **79:**6176–6179. http://dx.doi.org/10.1128/AEM.02015-13.
43. **Wang S, Huang H, Kahnt J, Thauer RK.** 2013. A reversible electron-bifurcating ferredoxin- and NAD-dependent [FeFe]-hydrogenase (HydABC) in *Moorella thermoacetica*. J Bacteriol **195:**1267–1275. http://dx.doi.org/10.1128/JB.02158-12.
44. **Weghoff MC, Bertsch J, Müller V.** 25 April 2014, posting date. A novel mode of lactate metabolism in strictly anaerobic bacteria. Environ Microbiol http://dx.doi.org/10.1111/1462-2920.12493.
45. **Ragsdale SW, Ljungdahl LG.** 1984. Purification and properties of NAD-dependent 5,10-methylenetetrahydrofolate dehydrogenase from *Acetobacterium woodii*. J Biol Chem **259:**3499–3503.
46. **Guenther BD, Sheppard CA, Tran P, Rozen R, Matthews RG, Ludwig ML.** 1999. The structure and properties of methylenetetrahydrofolate reductase from *Escherichia coli* suggest how folate ameliorates human hyperhomocysteinemia. Nat Struct Biol **6:**359–365. http://dx.doi.org/10.1038/7594.
47. **Kumagai H, Fujiwara T, Matsubara H, Saeki K.** 1997. Membrane localization, topology, and mutual stabilization of the *rnfABC* gene products in *Rhodobacter capsulatus* and implications for a new family of energy-coupling NADH oxidoreductases. Biochemistry **36:**5509–5521. http://dx.doi.org/10.1021/bi970014q.
48. **Pejchal R, Sargeant R, Ludwig ML.** 2005. Structures of NADH and CH_3-H_4folate complexes of *Escherichia coli* methylenetetrahydrofolate reductase reveal a Spartan strategy for a ping-pong reaction. Biochemistry **44:**11447–11457. http://dx.doi.org/10.1021/bi050533q.
49. **Bache R, Pfennig N.** 1981. Selective isolation of *Acetobacterium woodii* on methoxylated aromatic acids and determination of growth yields. Arch Microbiol **130:**255–261. http://dx.doi.org/10.1007/BF00459530.
50. **Daniel SL, Wu ZG, Drake HL.** 1988. Growth of thermophilic acetogenic bacteria on methoxylated aromatic acids. FEMS Microbiol Lett **52:**25–28. http://dx.doi.org/10.1111/j.1574-6968.1988.tb02566.x.
51. **Stupperich E, Konle R.** 1993. Corrinoid-dependent methyl transfer reactions are involved in methanol and 3,4-dimethoxybenzoate metabolism by *Sporomusa ovata*. Appl Environ Microbiol **59:**3110–3116.
52. **Maden BE.** 2000. Tetrahydrofolate and tetrahydromethanopterin compared: functionally distinct carriers in C_1 metabolism. Biochem J **350:**609–629. http://dx.doi.org/10.1042/0264-6021:3500609.
53. **Schuchmann K, Müller V.** 2013. Direct and reversible hydrogenation of CO_2 to formate by a bacterial carbon dioxide reductase. Science **342:**1382–1385. http://dx.doi.org/10.1126/science.1244758.
54. **Matthies D, Zhou W, Klyszejko AL, Anselmi C, Yildiz O, Brandt K, Müller V, Faraldo-Gomez JD, Meier T.** 2014. High-resolution structure and mechanism of an F/V-hybrid rotor ring in a Na^+-coupled ATP synthase. Nat Commun **5:**5286. http://dx.doi.org/10.1038/ncomms6286.